PHYSICAL REVIEW D **78,** 074026 (2008)

Top quark compositeness: Feasibility and implications

Alex Pomarol and Javi Serra

IFAE, Universitat Autònoma de Barcelona, 08193 Bellaterra, Barcelona

(Received 27 June 2008; published 29 October 2008)

In models of electroweak symmetry breaking in which the standard model fermions get their masses by mixing with composite states, it is natural to expect the top quark to show properties of compositeness. We study the phenomenological viability of having a mostly composite top. The strongest constraints are shown to mainly come from one-loop contributions to the T parameter. Nevertheless, the presence of light custodial partners weakens these bounds, allowing in certain cases for a high degree of top compositeness. We find regions in the parameter space in which the T parameter receives moderate positive contributions, favoring the electroweak fit of this type of model. We also study the implications of having a composite top at the LHC, focusing on the process $pp \to t\bar{t}t\bar{t}(b\bar{b})$ whose cross section is enhanced at high energies.

DOI: 10.1103/PhysRevD.78.074026 PACS numbers: 14.65.Ha, 12.60.Rc

I. INTRODUCTION

Unraveling the origin of the electroweak symmetry breaking (EWSB) is the main priority of the LHC. One possibility, inspired by QCD, is that EWSB occurs in a new strong sector at energies of few TeV. Examples of this realization are technicolor models [1] and composite Higgs scenarios [2]. More recently, due to the connection between strongly-coupled theories and gravity on warped extra dimensions, these scenarios have been studied in the framework of five-dimensional theories (see, for example, Refs. [3,4]).

In all these examples the standard model (SM) fields that get masses from EWSB must at least be coupled to this new (strong) sector with a strength proportional to their masses. This suggests that the top quark is the SM field with the largest coupling to the new sector, and therefore the most sensitive to new physics. If this is the case, the top is the most likely SM fermion to show signals of compositeness. Knowing the degree of compositeness of the top is then very important to understand the physics lying beyond the SM.

The aim of this paper is twofold. First, we want to study the viability of having a top quark being mostly a composite state. We will study this possibility in a framework, inspired by extra-dimensional models, in which the SM fermions are a mixture of elementary and composite states, with a mixing angle proportional to $\sqrt{m_f}$, where m_f is the fermion mass. We will take the limit in which one of the two chiral components of the top is mostly a composite state, and study the phenomenological viability of this limit. The main constraints from present experiments will arise from the T parameter. We will calculate the one-loop contributions to T and show under which conditions a composite top is allowed. An important role will be played by the custodial partners of the top, the custodians, that become light in the composite limit and reduce significantly the total contribution to T. Our results will also be useful to determine how a positive contribution to T can arise, as required, in this class of models, to accommodate a large and positive S parameter.

Second, we will show how future experiments can test the properties of the top and tell us about the degree of its compositeness. We will do this by following a model-independent approach, similar to Ref. [5], in which the top compositeness is characterized by few higher-dimensional operators. We will concentrate on the study of the process $pp \to t\bar{t}t\bar{t}(b\bar{b})$ that, for a composite top, is enhanced at high energies. We will calculate the cross section of this process and show how different observables can be used to distinguish between a composite and elementary top.

The organization of the paper is as follows. In Sec. II we present a framework for a composite top. Its low-energy effective Lagrangian is given in Sec. III. The experimental constraints are presented in Sec. IV; we study the effects on $Zb\bar{b}$ and the one-loop contributions to the T parameter. We present the regions of the parameter space in which a composite top is allowed. In Sec. V we show how to study the top properties at future experiments and present the calculation for $pp \to t\bar{t}t\bar{t}(b\bar{b})$. We conclude in Sec. VI.

II. FRAMEWORK

The framework we want to consider is the following. We will assume that beyond the SM there is a new sector (the BSM sector), characterized by two parameters, a generic coupling g_ρ, and a mass scale M_ρ. We will be mostly interested in the limit $1 < g_\rho \lesssim 4\pi$ such that the BSM sector consists of resonances whose coupling, although large, allows us for a perturbative expansion. Our analysis, however, will be able to be extended to the region $g_\rho \sim 4\pi$ corresponding to a maximally strongly-coupled BSM. The scale M_ρ, in analogy with QCD, will correspond to the mass of the lightest resonance. Examples of this class of models are strongly-coupled gauge theories in the large-N limit or extra-dimensional models [3,4].

We will also assume that this new sector is responsible for the EWSB. This means that the Goldstone bosons G^a (to be eaten by the W and Z) will arise from the BSM sector. They can be parametrized by a matrix Σ whose vacuum expectation value (VEV) breaks the electroweak symmetry

$$\Sigma = ve^{i\sigma^a G^a/v}, \quad \text{where } v \simeq 246 \text{ GeV}. \tag{1}$$

In Higgsless theories v is equal to the decay constants of the Goldstones f which can be written as

$$f = \frac{M_\rho}{g_\rho}. \tag{2}$$

In theories in which the Higgs arises from the BSM sector as a pseudo-Goldstone boson the scale f, satisfying Eq. (2), is associated to the pseudo-Goldstone boson-Higgs decay constant. The electroweak scale v is determined in these models by minimizing the Higgs potential and one generically obtains $v \lesssim f$ [2,4]. To incorporate both scenarios, Higgsless and composite Higgs, we will parametrize the deviation of v from f by the dimensionless parameter ξ defined by [5]

$$\xi = \frac{v^2}{f^2} \leq 1. \tag{3}$$

Electroweak precision tests (EWPT) put tight constraints on models of this class, since the BSM resonances induce sizable tree-level modifications of the SM gauge propagators. The main effects can be parametrized by two quantities, the S and T parameters [6]. The tree-level contribution to T can vanish if the BSM sector is invariant under a global $SU(2)_V$ symmetry, the so-called custodial symmetry. For this reason, we will assume that the BSM sector is invariant under a global $SU(2)_L \times SU(2)_R$ under which the Goldstone multiplet Σ transforms as a $(\mathbf{2}, \mathbf{2})$. The VEV of Σ will break $SU(2)_L \times SU(2)_R$ down to the diagonal subgroup corresponding to the custodial symmetry. We will further impose that the BSM sector is also invariant under the discrete symmetry P_{LR} that interchanges $L \leftrightarrow R$. As we will see later, this extra parity is crucial to avoid large corrections to $Zb\bar{b}$ [7]. Under these assumptions the only important tree-level constraint on this class of models comes from the S parameter. In extra-dimensional models in which S is calculable one finds, barring cancellations, the bound $M_\rho \gtrsim 2.3$ TeV[1] [4], or equivalently,

$$f \gtrsim 500 \text{ GeV} (\xi \lesssim 1/4) \quad \text{for } g_\rho \sim 4.6. \tag{4}$$

We could reduce the lower bound on f to reach the Higgsless limit $\xi = 1$, but at the prize of having a very large g_ρ. In this case the value of S can only be estimated, since it cannot be calculated by any perturbative method. In deriving Eq. (4) we have assumed that T receives a large and positive contribution, $\alpha \Delta T \sim 1$–4×10^{-3}, beyond that of the SM. As we will see later, this can arise from one-loop effects that can be sizable if the top is composite.

Finally, in the fermionic sector we will take the following extra assumption. The SM fermions will be assumed to be linearly coupled to the BSM resonances. This means that a basis exists in which the SM fermions couple to the BSM sector only through mass mixing terms. In particular, for the top we have

$$\begin{aligned} \mathcal{L} &= y_L f \bar{q}_L^{\text{el}} \mathcal{P}_q [Q_R] + y_R f \bar{t}_R^{\text{el}} \mathcal{P}_t [T_L] + M_Q \bar{Q}_L Q_R \\ &\quad + M_T \bar{T}_R T_L + g_\rho \bar{Q}_L \Sigma T_R + \cdots, \end{aligned} \tag{5}$$

where q_L^{el} and t_R^{el} denote the elementary left-handed top-bottom doublet and right-handed top, respectively, and $Q_{L,R}$ and $T_{L,R}$ are vectorlike "composite" BSM resonances. The operators $\mathcal{P}_q$ and $\mathcal{P}_t$ project the BSM resonances into components with the SM quantum numbers of q_L^{el} and t_R^{el}, respectively. We will consider that there is only one $Q_{L,R}$ and $T_{L,R}$ resonance. In five-dimensional theories this corresponds to keep only the lightest Kaluza-Klein state of each tower that it is usually a good approximation [8]. Apart from the mass terms, we have included in Eq. (5) the Yukawa term $\bar{Q}_L \Sigma T_R$, which is responsible, as we will see, for the top mass. The absence in Eq. (5) of bilinear couplings of elementary fields with the BSM resonances, e.g. $\bar{q}_L^{\text{el}} \Sigma t_R^{\text{el}}$, is a feature of holographic models [4]. It was also implemented in technicolor models in Ref. [9]. This implies that the top gets a mass through mixing with BSM states. This way of generating fermion masses is phenomenologically favorable, since it avoids dangerous flavor transitions [4] that were present in the original technicolor models. For our analysis here, however, the presence of terms like $\bar{q}_L^{\text{el}} \Sigma t_R^{\text{el}}$ would only introduce more parameters but would not qualitatively change our conclusions.

The SM-top components, q_L and t_R, are identified with the massless states (before EWSB). These are given by

$$\begin{aligned} q_L &= \cos\theta_L q_L^{\text{el}} + \sin\theta_L \mathcal{P}_q [Q_L], \qquad \tan\theta_L = \frac{y_L f}{M_Q}, \\ t_R &= \cos\theta_R t_R^{\text{el}} + \sin\theta_R \mathcal{P}_t [T_R], \qquad \tan\theta_R = \frac{y_R f}{M_T}. \end{aligned} \tag{6}$$

The orthogonal states get a mass squared $M_Q^2 + y_L^2 f^2$ and $M_T^2 + y_R^2 f^2$. The last term of Eq. (5) gives, after the above rotation, the Yukawa coupling of the top

$$y_t = g_\rho \sin\theta_L \sin\theta_R. \tag{7}$$

By requiring a top mass $m_t = y_t v \simeq 160$ GeV (at energies $M_\rho \sim 1$ TeV), Eq. (7) gives a lower bound for the mixing angles, $\sin\theta_{L,R} \gtrsim 0.6/g_\rho$. The largeness of these mixing angles makes natural the possibility that one of the two chiralities of the top is fully composite. We will consider this possibility below.

[1]Similar bound is obtained if we use the QCD experimental data to extract the value of S [6].

The top composite limit: We are interested in exploring the limit in which either $q_L^{\rm el}$ or $t_R^{\rm el}$ is maximally coupled to the BSM sector such that the SM q_L or t_R mostly corresponds to a composite BSM state. For the left-handed top, this corresponds to the limit

$$\left\{\begin{array}{c}\sin\theta_L \to 1\\ y_L \to g_\rho\end{array}\right\} \quad \text{and} \quad \left\{\begin{array}{c}\sin\theta_R \to y_t/g_\rho\\ y_R \simeq y_t\end{array}\right\}. \tag{8}$$

For the right-handed top, the composite limit is given by

$$\left\{\begin{array}{c}\sin\theta_R \to 1\\ y_R \to g_\rho\end{array}\right\} \quad \text{and} \quad \left\{\begin{array}{c}\sin\theta_L \to y_t/g_\rho\\ y_L \simeq y_t\end{array}\right\}. \tag{9}$$

In warped extra-dimensional models these limits can be obtained by taking negative values for the 5D mass of the left-handed (or right-handed) top that localizes the 4D massless state towards the IR boundary [4]. Although the composite limit can also be considered for other SM fermions, the fact that the top is the heaviest of all of them suggests that this is the most likely SM fermion to have one of its chiralities being mostly composite.

Let us concentrate for the moment on the q_L composite limit, Eq. (8). In this limit the SM left-handed top is part of the BSM multiplet Q_L. Since Q_L is in a $\mathrm{SU}(2)_L \times \mathrm{SU}(2)_R$ representation, the top will be accompanied by custodial partners, the custodians, corresponding to

$$(1 - \mathcal{P}_q)[Q_L] \equiv \tilde{\mathcal{P}}_q[Q_L]. \tag{10}$$

It is important to notice that the mass of the custodians is given by $M_Q = y_L f \cot\theta_L$ that in the composite limit tends to zero. Therefore in this limit the custodian states become lighter than the other resonances, $M_Q \ll M_\rho$. This effect has also been observed in 5D models in the limit in which the 5D masses take negative values and the massless states become localized towards the IR boundary [10]. Nevertheless, it is hard to understand what could be the origin of this new mass scale $M_Q \ll M_\rho$ in a generic strongly-coupled theory. The effect of having light custodians will have important phenomenological consequences as we will see later.

Similarly, in the right-handed top composite limit, Eq. (9), one finds that the custodians, given by $(1 - \mathcal{P}_t)[T_R] \equiv \tilde{\mathcal{P}}_t[T_R]$, are also light $M_T \ll M_\rho$.

From now on we will generically denote by q^* the custodians and by M_{q^*} their masses.

III. LOW-ENERGY EFFECTIVE LAGRANGIAN FOR A COMPOSITE TOP

At energies below the resonance masses, the effective theory corresponds to the SM plus higher-dimensional operators. These operators are induced by integrating out the heavy resonances at M_ρ and the custodians at M_{q^*}. In the first case, the higher-dimensional operators are suppressed by M_ρ. Among these operators, we will be interested in those carrying extra powers of g_ρ such that the effective scale that suppresses these operators is in fact $g_\rho/M_\rho = 1/f$, that in the limit considered here $g_\rho > 1$, is larger than $1/M_\rho$. These are operators with extra composite tops or Higgs fields (or, in Higgsless theories, the Goldstones) which couple to the BSM resonances with a coupling of order g_ρ. Let us present the list of these operators for the case of a composite q_L, Eq. (8). Up to order p^2/f^2, we have three dimension-six operators of this type [5]

$$\frac{ic_L^{(1)}}{f^2} H^\dagger D_\mu H \bar{q}_L \gamma^\mu q_L + \frac{ic_L^{(3)}}{2f^2} H^\dagger \sigma^i D_\mu H \bar{q}_L \gamma^\mu \sigma^i q_L + \text{H.c.} + \frac{c_{4q}}{f^2}(\bar{q}_L \gamma^\mu q_L)(\bar{q}_L \gamma_\mu q_L). \tag{11}$$

We are using the two-component notation H for the Higgs multiplet

$$\Sigma = (\tilde{H}, H) \quad \text{where } H^\dagger H = v^2, \tag{12}$$

and $\tilde{H} = i\sigma_2 H^*$. Notice that we are only including in H the Goldstones and not the Higgs particle. The effects of a composite Higgs were already studied in Ref. [5]. In the case where $v = f$, we cannot expand in H/f, and we have, at the same leading order as the first two operators of Eq. (11), a dimension-eight operator

$$\frac{ic_L'}{f^4} H^\dagger D_\mu H (\bar{q}_L H) \gamma^\mu (H^\dagger q_L). \tag{13}$$

The second class of operators that we will be interested in are those induced by integrating out the custodians. These operators are suppressed by M_{q^*}. Since the q_L's custodial partners do not mix with q_L (they have different quantum numbers), operators induced at tree level cannot contain q_L. The custodians of q_L, however, can mix with t_R through the Yukawa coupling generating higher-dimensional operators involving t_R and H and carrying powers of $y_t^2/M_{q^*}^2$. The leading operator of this kind is given by

$$\frac{i\tilde{c}_R y_t^2}{M_{q^*}^2} H^\dagger D_\mu H \bar{t}_R \gamma^\mu t_R. \tag{14}$$

At this point it is worth emphasizing the crucial difference between the two classes of operators, Eq. (11) and (14). The origin of the operator in Eq. (14) is the mixing of t_R with the custodians. Therefore the strength of this operator is related to the lightness of these extra states. On the other hand, the strength of the operators in Eq. (11) measures the degree of compositeness of the top that do not have to be related to new light degrees of freedom.

We can repeat the same analysis for the case of a composite t_R. Up to order p^2/f^2, we have two operators [5]

$$\frac{ic_R}{f^2} H^\dagger D_\mu H \bar{t}_R \gamma^\mu t_R + \frac{c_{4t}}{f^2}(\bar{t}_R \gamma^\mu t_R)(\bar{t}_R \gamma_\mu t_R), \tag{15}$$

while at order $p^2/M_{q^*}^2$ we have (from integrating out the custodians of t_R)

$$\frac{i\tilde{c}_L^{(1)} y_t^2}{M_{q^*}^2} H^\dagger D_\mu H \bar{q}_L \gamma^\mu q_L + \frac{i\tilde{c}_L^{(3)} y_t^2}{2M_{q^*}^2} H^\dagger \sigma^i D_\mu H \bar{q}_L \gamma^\mu \sigma^i q_L + \text{H.c.} \quad (16)$$

The coefficients c_i are $\mathcal{O}(1)$ constants whose values depend on the details of the BSM sector. In certain cases, as we will see, these coefficients fulfill certain relations due to the underlying symmetries of the BSM. For a composite Higgs model the values of $c_{R,L}$ are given in Ref. [7]. In these models the four-fermion interactions arise from integrating out heavy vector resonances. From a color resonance, assuming a coupling g_ρ to the top, one has

$$c_{4t} = c_{4q} = -\tfrac{1}{6}, \quad (17)$$

while for a singlet resonance one gets $c_{4t} = c_{4q} = -1/2$.

IV. PRESENT EXPERIMENTAL CONSTRAINTS

In this section we want to study how much the present experimental data limits the compositeness of the top. Although important effects of the top compositeness could be revealed in flavor physics, we will not discuss them here (see, however, Ref. [5]). These effects strongly depend on the underlying theory of flavor, and therefore are very model dependent. Discarding flavor physics, the most stringent bound on the composite q_L case comes from $Zb_L\bar{b}_L$ that has been measured at LEP at the per mille level. This bound has been strongly disfavored in the past technicolor models and other variants [11]. From the Lagrangian of Eq. (11), we find a deviation from the SM $Zb_L\bar{b}_L$ coupling given by

$$\frac{\delta g_{b_L}}{g_{b_L}} = \frac{(c_L^{(1)} + c_L^{(3)})\xi}{1 - \frac{2}{3}\sin^2\theta_W}. \quad (18)$$

For $c_L^{(1),(3)} \sim 1$, as expected for a composite q_L, Eq. (18) gives a large deviation, excluded by the present LEP data. This strong bound, however, can be evaded in certain custodial BSM models. As pointed out in Ref. [7], the custodial symmetry implemented with P_{LR} (that interchanges $L \leftrightarrow R$) can protect $Zb\bar{b}$ from large deviations from its SM value. This occurs when the BSM field that couples to b_L has the following isospin-left and isospin-right charge assignments [7]:

$$T_L = T_R = 1/2, \qquad T_L^3 = T_R^3 = -1/2. \quad (19)$$

In this case one finds, from integrating out the BSM sector, $c_L^{(1)} = -c_L^{(3)}$, and therefore no contributions to Eq. (18) are generated. The only effect on $Zb\bar{b}$ will arise from loops involving SM particles (together with BSM states) that do not respect the custodial and P_{LR} symmetry. We will comment on these effects later on.

TABLE I. Charge assignments for the states Q and T under $\mathrm{SU}(2)_L \times \mathrm{SU}(2)_R \times U(1)_X$.

	Q	T
Case (a)	$(2, 2)_{2/3}$	$(1, 1)_{2/3}$
Case (b)	$(2, 2)_{2/3}$	$(1, 3)_{2/3} + (3, 1)_{2/3}$

Assuming that Eq. (19) is fulfilled, and that the operator $\bar{Q}_L \Sigma T_R$ must be allowed to give masses to the SM fermions, we are left with only two possible charge assignments for the states Q and T under $\mathrm{SU}(2)_L \times \mathrm{SU}(2)_R \times \mathrm{U}(1)_X$,[2] given in Table I. In this article we will concentrate only on these two possibilities.

A. The $\hat{T}$ parameter

With $Zb\bar{b}$ under control at tree level, the next important observable is the T parameter. The contribution to T arises from the higher-dimensional operator

$$\frac{c_T}{2f^2}|H^\dagger D_\mu H|^2, \qquad \hat{T} = c_T \xi, \quad (20)$$

where we follow the notation of Ref. [12] in which the T parameter is rescaled: $\hat{T} = \alpha T \simeq T/129$. As we previously said, $\hat{T}$ is zero at the tree level by the custodial symmetry. Nevertheless, it can be generated at the one-loop level due to the $y_{L,R}$ couplings in Eq. (5) which break the custodial symmetry. A dimensional estimate shows that [5]

$$\hat{T} \sim \frac{N_c}{16\pi^2}\left(\frac{y_{L,R}}{g_\rho}\right)^4 \frac{\xi\Lambda^2}{f^2}, \quad (21)$$

where $N_c = 3$ is the QCD number of colors and Λ is the cutoff scale. If $\Lambda \sim M_\rho$ we get a very large contribution, forbidding the composite region $y_{L,R} \sim g_\rho$. Nevertheless, we must recall that in the top composite limit, the custodians are light $M_{q^*} < M_\rho$, and, as we will see, are their masses what really cut off the loop momentum. Therefore we cannot neglect the effects of the custodians Q and T that can diminish the bound on $y_{L,R}$ and allow a higher degree of compositeness for the top.

We have performed the calculation of $\hat{T}$ in the q_L and t_R composite limits taking into account the custodians. We have considered the two charge assignments (a) and (b) of Table I. For a composite q_L the results of $\hat{T}$ are plotted in Figs. 2 and 4 for the charge assignment (a) and (b), respectively. They depend on the mass of the custodians, M_{q^*}, and the coefficient of the higher-dimensional operator $c_L \equiv c_L^{(3)} = -c_L^{(1)}$. For a composite t_R, only the charge assignment (b) gives a nonzero contribution to $\hat{T}$. This is plotted in Fig. 6. In this case the constraints on $\hat{T}$ do not

[2]The extra global $\mathrm{U}(1)_X$ symmetry of the BSM sector is needed to properly embed the hypercharge of the SM, $Y = T_R^3 + X$.

give any direct bound on the coefficients c_i of Eq. (15), but only on the coefficient of the higher-dimensional operators of the custodians c_R'.

To understand these results we will present the calculation of $\hat{T}$ in the limit $M_\rho \gg M_{q^*} \gg m_t$ following the effective theory approach of Ref. [13]. This consists in calculating the leading effects to $c_T(\mu)$ at the three different values of the renormalization scale μ: at $M_{q^*} < \mu < M_\rho$ in the effective theory after integrating out the heavy resonances, at $m_t < \mu < M_{q^*}$ after integrating out the custodians, and finally at $\mu < m_t$ after integrating out the top.

Let us start with the q_L composite limit:

Case (a): The theory below M_ρ but above M_{q^*} consists of the SM plus the custodians. The q_L and its custodians q_L^* are embedded in the $(\mathbf{2},\mathbf{2})_{\mathbf{2/3}}$ representation denoted by Q_L. Under the SM $\mathrm{SU}(2)_L \times \mathrm{U}(1)_Y$ group, q_L^* transforms as a $\mathbf{2_{7/6}}$. We choose to represent Q_L by a 2×2 matrix given by $Q_L = (q_L, q_L^*)$. The dimension-four operators involving the top and the custodians are given by

$$\mathcal{L}_4 = \mathrm{Tr}[\bar{Q}_L i\not{D} Q_L] + \mathrm{Tr}[\bar{Q}_R i\not{D} Q_R \tilde{P}_q] + \bar{t}_R i\not{D} t_R + \{y_t \mathrm{Tr}[\bar{Q}_L \Sigma P_t^{-1}] t_R + M_{q^*} \mathrm{Tr}[\bar{Q}_L Q_R \tilde{P}_q] + \mathrm{H.c.}\}, \tag{22}$$

where $P_t^{-1} = 1$ follows from the embedding $T_R \equiv (\mathbf{1},\mathbf{1})$ and $\tilde{P}_q = (1-\sigma_3)/2$. Notice that the only breaking of the custodial symmetry arises from the custodian mass term due to the presence of $\tilde{P}_q$. There are also dimension-six operators that can contribute to $\hat{T}$. Up to order p^2/f^2, they are given by

$$\mathcal{L}_6 = \frac{c_L}{f^2}\{\mathrm{Tr}[\bar{Q}_L \gamma^\mu Q_L \hat{V}_\mu] + \mathrm{Tr}[\bar{Q}_L \gamma^\mu V_\mu Q_L]\}, \tag{23}$$

where c_L is a coefficient of order one and we have defined $V_\mu = (iD_\mu \Sigma)\Sigma^\dagger$, $\hat{V}_\mu = (iD_\mu\Sigma)^\dagger \Sigma$, and the covariant derivative is given by $D_\mu \Sigma = \partial_\mu \Sigma - ig\sigma_a W_\mu^a \Sigma/2 + ig' B_\mu \Sigma \sigma_3/2$. We are omitting the double-trace operator $\mathrm{Tr}[\bar{Q}_L i\not{D}\Sigma]\mathrm{Tr}[\Sigma^\dagger Q_L]$ since this is suppressed in 5D theories [7] or strongly-coupled theories in the large-N limit. The fact that the two operators in Eq. (23) have equal coefficients is a consequence of the P_{LR} symmetry. We are neglecting operators suppressed by $M_{q^*}^2/M_\rho^2$ that we consider small in the top composite limit.

At the order that we are working, the coefficient c_T does not receive any contribution from integrating out the resonances at M_ρ.[3] To see this, notice that the one-loop contribution to $\hat{T}$ arising from the effective Lagrangian Eqs. (22) and (23) is finite, i.e., insensitive to the cutoff M_ρ. This is a consequence of the custodial symmetry. Indeed, the parameter $\hat{T}$, that transforms as a **5** under the custodial $\mathrm{SU}(2)_V$ [14], can only be generated from diagrams with at least four M_{q^*} insertions, since M_{q^*} transforms as a **2** under $\mathrm{SU}(2)_V$ (as a $(\mathbf{1},\mathbf{2})$ under $\mathrm{SU}(2)_L \times \mathrm{SU}(2)_R$). This renders the custodian loop diagrams to $\hat{T}$ finite.[4] Our explicit calculation below will confirm this expectation.

Let us now integrate out the custodians. Apart from SM terms, this generates the effective Lagrangian terms of Eqs. (11) and (14) with the coefficients

$$c_L^{(3)} = -c_L^{(1)} = c_L, \qquad c_L' = 0, \qquad \tilde{c}_R = 1. \tag{24}$$

To obtain the coefficient c_T at the custodian mass scale we must use the matching condition at this boundary $\mu = M_{q^*}$ which is given by

$$\hat{T}_{\text{total}} = \hat{T}_{\text{custodians}} + \hat{T}_{\text{top}} + \hat{T}_{\text{mix}} = c_T(M_{q^*})\xi + \hat{T}_{\text{top}}, \tag{25}$$

where $\hat{T}_{\text{total}}$ includes the contributions from all the scales to the $\hat{T}$ parameter, and $\hat{T}_{\text{custodians}}$, $\hat{T}_{\text{top}}$, and $\hat{T}_{\text{mix}}$ includes, respectively, those arising from loops of custodians, tops, and both. $\hat{T}_{\text{top}}$ drops in Eq. (25) since we are not yet integrating out the top. The three contributions, $\hat{T}_{\text{custodians}}$, $\hat{T}_{\text{top}}$, and $\hat{T}_{\text{mix}}$, separately, are understood as being renormalized in the $\overline{\text{MS}}$ scheme. Therefore, our matching condition for c_T becomes

$$\xi c_T(M_{q^*}) = \hat{T}_{\text{top}}^{\text{SM}}\left(2c_L^2 \frac{\xi^2}{\epsilon_t} + 6c_L^2\xi^2 + 8c_L\xi + \frac{22}{3}\epsilon_t\right), \tag{26}$$

where we have kept the leading and subleading terms in the expansion parameter

$$\epsilon_t = \frac{m_t^2}{M_{q^*}^2} \ll 1, \tag{27}$$

and we have defined $\hat{T}_{\text{top}}^{\text{SM}}$ as

$$\hat{T}_{\text{top}}^{\text{SM}} = \frac{3m_t^2}{16\pi^2 v^2} \simeq 0.008, \tag{28}$$

that is equal to the SM-top leading contribution to $\hat{T}$. It is important to note that all except the first term in the right-hand side of Eq. (26) are scheme dependent. This first term shows that, as expected, the quadratic divergence scale of Eq. (21) is replaced by $M_{q^*}^2$.

Now, we must use the renormalization group to scale $c_T(M_{q^*})$ down to the lower scale m_t, where we can inte-

[3] We are not considering the contribution coming from a loop of gauge bosons.

[4] This does not mean that the custodian contribution to $\hat{T}$ must be proportional to $M_{q^*}^4$. Diagrams with four M_{q^*} insertions contributing to $\hat{T}$ are UV finite but infrared divergent $\hat{T} \propto M_{q^*}^4/\Lambda_{IR}^2$. The infrared divergence is cure by the same M_{q^*} when resumming over all possible M_{q^*} insertions, giving a final contribution $\hat{T} \propto M_{q^*}^2$. Similar argument explains the finiteness of the SM-top contribution to $\hat{T}$ and its proportionality to m_t^2.

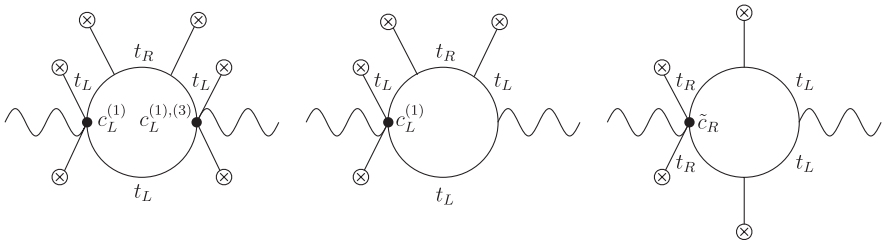

FIG. 1. Logarithmic divergent loop diagrams contributing to the SM gauge boson masses, and therefore to c_T, for the low-energy effective theory of a composite q_L, Eqs. (11) and (14). The external lines with a cross correspond to insertions of the Higgs VEV.

grate out the top quark. The leading logarithmic terms arise from the diagrams of Fig. 1. We obtain the equation

$$\xi c_T(m_t) = \xi c_T(M_{q^*}) + \hat{T}^{\rm SM}_{\rm top}(6c_L^2\xi^2 + 4c_L\xi + 4\tilde{c}_R\epsilon_t)\log\epsilon_t. \tag{29}$$

Finally, we must integrate out the top. The matching condition at the boundary $\mu = m_t$ is given by

$$[\xi c_T(\mu) + \hat{T}_{\rm top}]_{\mu\to m_t^+} = [\xi c_T(\mu)]_{\mu\to m_t^-}, \tag{30}$$

where in the $\overline{\rm MS}$ scheme

$$[\hat{T}_{\rm top}]_{\mu\to m_t^+} = \hat{T}^{\rm SM}_{\rm top}(c_L^2\xi^2 + 2c_L\xi). \tag{31}$$

Here we are not including the SM-top contribution to c_T since we want only the contribution to $\hat{T}$ beyond the one of the SM. Adding up Eqs. (26), (29), and (31) we obtain

$$\begin{aligned}\hat{T} &= \xi c_T(0)\\ &= \hat{T}^{\rm SM}_{\rm top}\Big[c_L^2\xi^2\Big(\frac{2}{\epsilon_t} + 7 + 6\log\epsilon_t\Big) + c_L\xi(10 + 4\log\epsilon_t)\\ &\quad + \epsilon_t\Big(\frac{22}{3} + 4\log\epsilon_t\Big)\Big].\end{aligned} \tag{32}$$

As explained before, this result is valid in the limit $M_\rho \gg M_{q^*} \gg m_t$. We have checked that in this limit it agrees with the exact calculation.

In Fig. 2 we present a plot of $\hat{T}$ (the exact result) in the $M_{q^*} - c_L\xi/\xi_R$ plane, where $\xi_R = 1/4$ is the reference value of ξ in composite Higgs models—see Eq. (4). The gray area shows the region $-1.7\times10^{-3} < \hat{T} < +1.9\times10^{-3}$ and the dashed lines show the contribution to $|\hat{T}|$ equal to 2.8, 4.2, and 5.6 as they, respectively, move away from the gray area; we have marked with a "+" ("−") the areas in which the contribution to $\hat{T}$ is positive (negative). We see that the region of a composite top, $c_L\xi/\xi_R \sim 1$, is allowed although, as we expected, requires light custodians $M_{q^*} \lesssim 1$ TeV. This correlation between M_{q^*} and c_L tells us that the custodians must be seen at the LHC if q_L is a fully composite state. Figure 2 also shows the region in which $\hat{T}$ gets a positive contribution, as needed in composite Higgs or Higgsless models in order to satisfy EWPT. We see that a positive contribution $\hat{T} \sim 1$–4×10^{-3} is easily achieved for a composite top, especially for negative values of c_L and large values of the custodian mass. For small values of M_{q^*}, we obtain however a negative value for $\hat{T}$ that can be easily understood as follows. In the Lagrangian Eqs. (22) and (23) the scale M_{q^*} is the only breaking parameter of the custodial symmetry. Therefore in the limit $M_{q^*} \to 0$ we must get that the total contribution of the top and custodian sector must be zero, implying that the custodian contribution is given by $\hat{T} = -\hat{T}^{\rm SM}_{\rm top} < 0$. In Fig. 2 we also show, with a dotted line, the prediction for the holographic Higgs model [10] in which $\xi \sim 1/4$ and $M_{q^*} \sim 2.3\sqrt{1-2c_L}$ TeV. Notice that in this model the contribution to $\hat{T}$ is negative, as it is also shown in Ref. [15].

Case (b): In this case the representation of T_R is $(\mathbf{1},\mathbf{3})_{\mathbf{2/3}} + (\mathbf{3},\mathbf{1})_{\mathbf{2/3}}$ that implies that the low-energy effec-

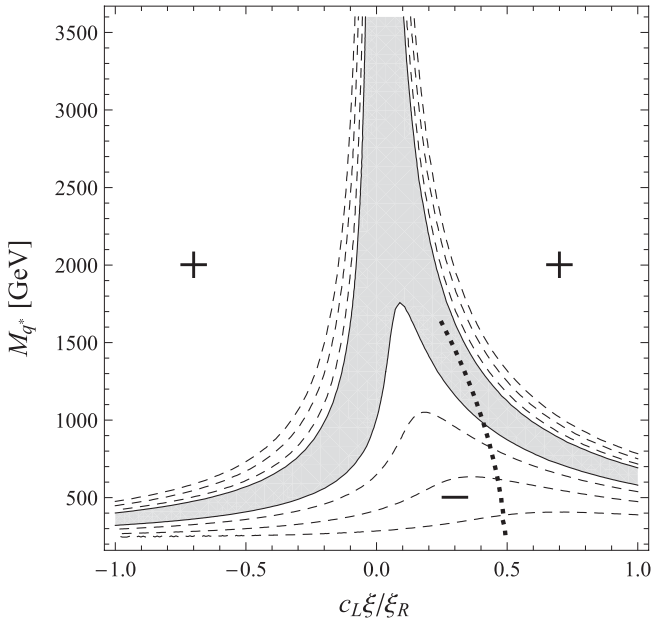

FIG. 2. Contribution to $\hat{T}$ in the q_L composite limit [case (a)] in the $M_{q^*} - c_L\xi/\xi_R$ plane, where $\xi_R = 1/4$. The gray area shows the region $-1.7\times10^{-3} < \hat{T} < +1.9\times10^{-3}$ and the dashed lines show the contribution to $|\hat{T}|$ equal to 2.8, 4.2, and 5.6 as they, respectively, move away from the gray area. We have marked with a "+" ("−") the areas in which the contribution to $\hat{T}$ is positive (negative). The dotted line corresponds to the holographic composite Higgs model.

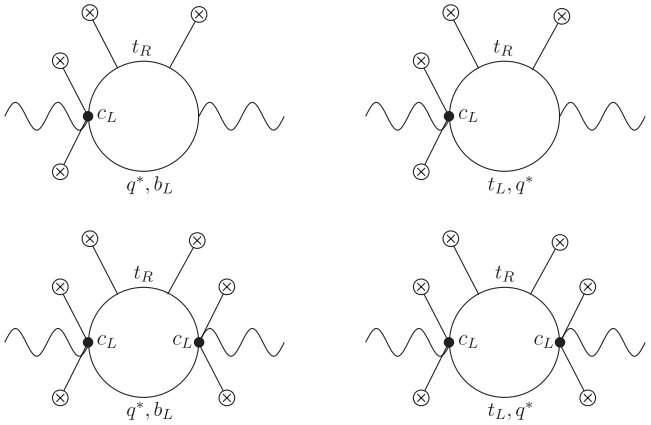

FIG. 3. Logarithmic divergent loop diagrams contributing to the SM gauge boson masses, and therefore to c_T, for the low-energy effective theory of a composite q_L and its custodians [case (b)]. The external lines with a cross correspond to insertions of the Higgs VEV.

tive Lagrangian for the top and the custodians below M_ρ is the same as that of Eqs. (22) and (23) but with $P_t^{-1} = \sigma_3$. Now the breaking of the custodial symmetry not only comes from the custodian mass term but also from the Yukawa coupling.[5] This implies that, contrary to case (a), the one-loop contribution to c_T is not finite. Indeed, the Yukawa coupling transforms as a **3** under the custodial symmetry $SU(2)_V$, and therefore contributions to $\hat{T}$ [a **5** of $SU(2)_V$] only need two powers of y_t. In this case, as shown in Fig. 3, there are custodian diagrams contributing to $\hat{T}$ that are logarithmically UV divergent.

We have now $c_T(M_\rho) \propto y_t^2$ that, being sensitive to the physics at M_ρ, cannot be predicted within our effective Lagrangian approach. What it is calculable, however, is the evolution of the coefficient $c_T(\mu)$ from $\mu = M_\rho$ to $\mu = M_{q^*}$ that comes from the diagrams of Fig. 3. We obtain

$$\xi c_T(M_{q^*}) = \xi c_T(M_\rho) - \hat{T}^{\rm SM}_{\rm top} 16 (c_L^2 \xi^2 + c_L \xi) \log(M_\rho^2/M_{q^*}^2). \tag{33}$$

From now on we will define M_ρ by the scale at which $c_T(M_\rho) = 0$. Let us now integrate out the custodians. The coefficients of the effective Lagrangian of the top are the same as those in Eq. (24). For c_T, the matching condition at $\mu = M_{q^*}$ reads

$$[\xi c_T(\mu)]_{\mu \to M_{q^*}^-} = [\xi c_T(\mu) + \hat{T}_{\rm custodians} + \hat{T}_{\rm mix}]_{\mu \to M_{q^*}^+}, \tag{34}$$

where

$$[\hat{T}_{\rm custodians} + \hat{T}_{\rm mix}]_{\mu = M_{q^*}^+} = \hat{T}^{\rm SM}_{\rm top} \left(2 c_L^2 \frac{\xi^2}{\epsilon_t} + 6 c_L^2 \xi^2 - 8 c_L \xi + \frac{22}{3} \epsilon_t \right). \tag{35}$$

Including the evolution of c_T from M_{q^*} to m_t and integrating out the top, that proceeds exactly as in the previous case, we end up with

$$\hat{T} = \hat{T}^{\rm SM}_{\rm top} \left[c_L^2 \xi^2 \left(\frac{2}{\epsilon_t} + 7 + 6 \log \epsilon_t - 16 \log \frac{M_\rho^2}{M_{q^*}^2} \right) + c_L \xi \left(-6 + 4 \log \epsilon_t - 16 \log \frac{M_\rho^2}{M_{q^*}^2} \right) + \epsilon_t \left(\frac{22}{3} + 4 \log \epsilon_t \right) \right]. \tag{36}$$

The exact value of $\hat{T}$ in the $M_{q^*} - c_L \xi / \xi_R$ plane is presented in Fig. 4 for $M_\rho \simeq 2.3$ TeV (left) and $M_\rho \simeq 3.6$ TeV (right). The region of sizable values of $c_L \xi / \xi_R$ is extremely reduced due to the logarithms of Eq. (33), disfavoring the possibility of a composite q_L in this case. This analysis, however, is useful to show that regions with positive contributions to $\hat{T}$ are quite generic; they correspond to $c_L < 0$. Since previous studies of the effects of $\hat{T}$ [15] centered in minimal holographic models in which $c_L > 0$, these regions with positive $\hat{T}$ were overlooked.

Let us now consider the t_R composite limit:

Case (a): In this case T_R is a singlet that corresponds, in the limit Eq. (9), to t_R. There are no custodians and the effective theory below M_ρ corresponds to the SM plus the operators of Eqs. (15). We find

$$c_R = 0, \tag{37}$$

that is a consequence of the custodial symmetry [7]. Equation (37) together with the absence of custodians imply that $\hat{T}$ is not generated at the order considered here. Hence, no serious bounds on a composite t_R are obtained in this case.

Case (b): In this case $t_R \in T_R^{(1)} + T_R^{(2)}$ transforming as a $(\mathbf{1}, \mathbf{3})_{\mathbf{2/3}} + (\mathbf{3}, \mathbf{1})_{\mathbf{2/3}}$. There are then five custodians that transform as $\mathbf{1}_{\mathbf{5/3}}$, $\mathbf{1}_{\mathbf{-1/3}}$, and $\mathbf{3}_{\mathbf{2/3}}$ under the electroweak symmetry. Using a 2×2 matrix representation for $T_R^{(1),(2)}$, we have the following dimension-four operators for the top and custodians

$$\begin{aligned} \mathcal{L}_4 = {} & {\rm Tr}[\bar{T}_R^{(1)} i \not{D} T_R^{(1)}] + {\rm Tr}[\bar{T}_R^{(2)} i \not{D} T_R^{(2)}] + {\rm Tr}[\bar{T}_L^{(1)} i \not{D} T_L^{(1)}] \\ & + {\rm Tr}[\bar{T}_L^{(2)} i \not{D} T_L^{(2)}] + \bar{q}_L i \not{D} q_L \\ & + y_t \sqrt{2}\, {\rm Tr}[(\bar{T}_R^{(1)} \Sigma^\dagger + \Sigma^\dagger \bar{T}_R^{(2)}) \mathcal{P}_q^{-1}(q_L)] \\ & + M_{q^*} \{ {\rm Tr}[\bar{T}_R^{(1)} \tilde{P}_t T_L^{(1)}] + {\rm Tr}[\bar{T}_R^{(2)} T_L^{(2)}] \} + {\rm H.c.}, \end{aligned} \tag{38}$$

where $\mathcal{P}_q^{-1}(q_L) = (q_L, 0)$ and $\tilde{P}_t = \sigma_3$. These two projectors, appearing in the Yukawa and custodian masses, pa-

[5] This latter breaking arises from the fact that $y_R \simeq y_t$ in Eq. (5) breaks the custodial symmetry.

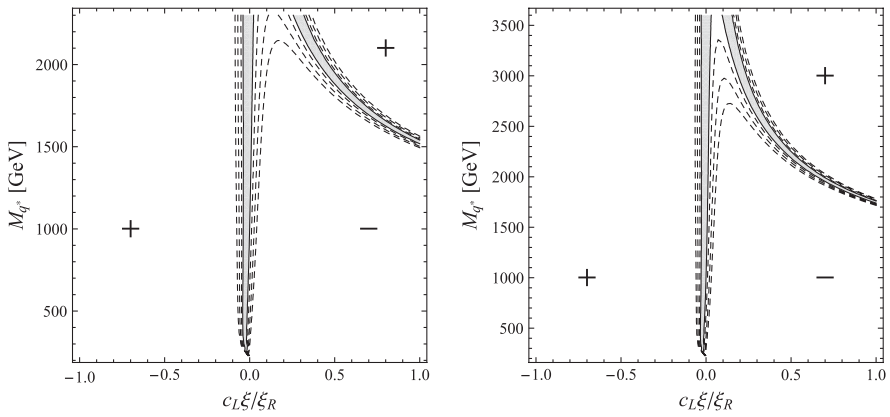

FIG. 4. Contribution to $\hat{T}$ in the q_L composite limit [case (b)] in the $M_{q^*} - c_L\xi/\xi_R$ plane, where $\xi_R = 1/4$. The gray area shows the region $-1.7 \times 10^{-3} < \hat{T} < +1.9 \times 10^{-3}$ and the dashed lines show the contribution to $|\hat{T}|$ equal to 2.8, 4.2, and 5.6 as they, respectively, move away from the gray area. We have marked with a "+" ("−") the areas in which the contribution to $\hat{T}$ is positive (negative). We have taken $M_\rho = 2.3$ TeV (left) and $M_\rho = 3.6$ TeV (right).

rametrize the breaking of the custodial symmetry. Contributing to $\hat{T}$, there can also be dimension-six operators that, up to order p^2/f^2, are given by

$$\frac{c_R'}{f^2}\{\mathrm{Tr}[\bar{T}_R^{(1)}\gamma^\mu[\hat{V}_\mu, T_R^{(1)}]] - \mathrm{Tr}[\bar{T}_R^{(2)}\gamma^\mu[V_\mu, T_R^{(2)}]]\}. \quad (39)$$

The contribution of the above Lagrangian to c_T is logarithmically divergent.[6] The divergence is generated by the diagrams of Fig. 5; they give us the evolution of c_T from M_ρ to M_{q^*}. Again, choosing the scale M_ρ such that $c_T(M_\rho) = 0$, we have

$$\xi c_T(M_{q^*}) = -\hat{T}_{\mathrm{top}}^{\mathrm{SM}} 2c_R'^2\xi^2\frac{1}{\epsilon_t}\log(M_\rho^2/M_{q^*}^2). \quad (40)$$

Let us now integrate the custodians. We are led to the Lagrangian Eqs. (15) and (16) with the coefficients

$$c_R = 0, \qquad \tilde{c}_L^{(1)} = -\tilde{c}_L^{(3)} = \tfrac{1}{2}. \quad (41)$$

As in the previous case, we have $c_R = 0$ due to the custodial symmetry [7]. For c_T, the matching at $\mu = M_{q^*}$ is given by Eq. (34) where

$$[\hat{T}_{\mathrm{custodians}} + \hat{T}_{\mathrm{mix}}]_{\mu\to M_{q^*}^+} = \hat{T}_{\mathrm{top}}^{\mathrm{SM}}\left(c_R'^2\frac{\xi^2}{\epsilon_t} + 4c_R'^2\xi^2 - 8c_R'\xi - \frac{16}{3}\epsilon_t\right). \quad (42)$$

The running from M_{q^*} to m_t proceeds by the same diagrams as those in Fig. 1 but with the replacements $\tilde{c}_R \to c_R\xi/\epsilon_t$ and $c_L^{(1),(3)} \to \tilde{c}_L^{(1),(3)}\epsilon_t/\xi$. We obtain

$$\xi c_T(m_t) = \xi c_T(M_{q^*}) + \hat{T}_{\mathrm{top}}^{\mathrm{SM}}(-2\epsilon_t)\log\epsilon_t. \quad (43)$$

Finally, when we match at the top mass scale, Eq. (30), we get

$$[\hat{T}_{\mathrm{top}}]_{\mu\to m_t^+} = \hat{T}_{\mathrm{top}}^{\mathrm{SM}}(-\epsilon_t). \quad (44)$$

Again, we are not including the SM-top contribution. Adding Eqs. (40) and (42)–(44), we obtain the total contribution to $\hat{T}$

$$\hat{T} = \hat{T}_{\mathrm{top}}^{\mathrm{SM}}\left[c_R'^2\xi^2\left(\frac{1}{\epsilon_t} + 4 - \frac{2}{\epsilon_t}\log\frac{M_\rho^2}{M_{q^*}^2}\right) - 8c_R'\xi - \epsilon_t\left(\frac{19}{3} + 2\log\epsilon_t\right)\right]. \quad (45)$$

A plot of the value of $\hat{T}$ is presented in Fig. 6 in the $M_{q^*} - c_R'\xi/\xi_R$ plane for $M_\rho = 2.3$ TeV and 3.6 TeV. We note that the parameter c_R' is not related to any coefficient of the low-energy top Lagrangian. Nevertheless, since one expects $c_R'\xi/\xi_R$ to be of order 1 for a composite t_R, the bounds from Fig. 6 can be considered indirect limits on the degree of compositeness of t_R. These bounds are strong in the

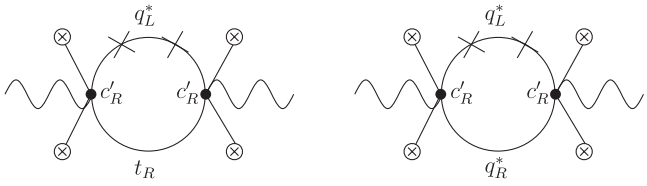

FIG. 5. Logarithmic divergent loop diagrams contributing to the SM gauge boson masses, and therefore to c_T, for the low-energy effective theory of a composite t_R and its custodial partners [case (b)]. The external lines with a cross correspond to insertions of the Higgs VEV and the crosses denote M_{q^*} insertions.

[6] We can see this by assigning to y_t and M_{q^*} the representation $(\mathbf{1}, \mathbf{2})$ and $(\mathbf{1}, \mathbf{3})$, respectively, to make the Lagrangian $\mathrm{SU}(2)_L \times \mathrm{SU}(2)_R$ invariant. Therefore $\hat{T}$ must arise from diagrams with four powers of y_t and two of M_{q^*}. The diagrams with two M_{q^*} insertions (Fig. 5) are logarithmically UV divergent.

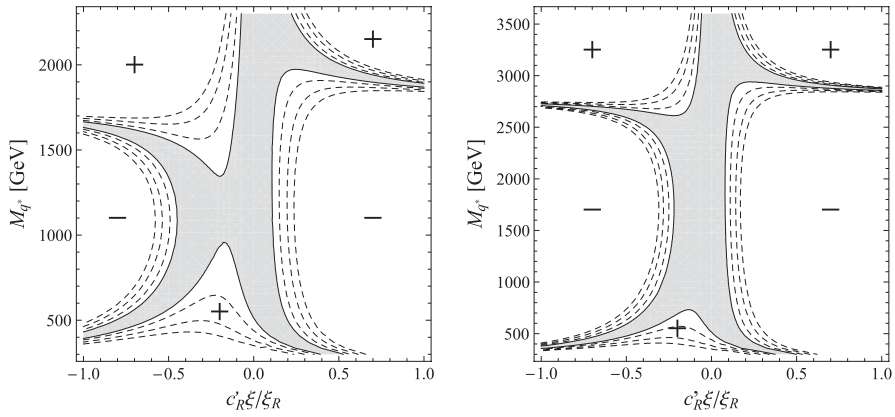

FIG. 6. Contribution to $\hat{T}$ in the t_R composite limit [case (b)] in the $M_{q^*} - c'_R\xi/\xi_R$ plane, where $\xi_R = 1/4$. The gray area shows the region $-1.7 \times 10^{-3} < \hat{T} < +1.9 \times 10^{-3}$ and the dashed lines show the contribution to $|\hat{T}|$ equal to 2.8, 4.2, and 5.6 as they, respectively, move away from the gray area. We have marked with a "+" ("−") the areas in which the contribution to $\hat{T}$ is positive (negative). We have taken $M_\rho = 2.3$ TeV (left) and $M_\rho = 3.6$ TeV (right).

$c'_R > 0$ region, but quite weak for $c'_R < 0$. It is interesting to see that in this latter region it is very natural to have a positive contribution to $\hat{T}$, as needed for EWPT.

From the above analysis we can summarize the following. A composite q_L is only likely in case (a). It yields to $c_L^{(1)} = -c_L^{(3)} \sim 1$ so it can be tested in modifications of the top couplings. On the other hand, a composite t_R is weakly constrained in both cases. Case (a) predicts a small $\hat{T}$, while in case (b) $\hat{T}$ can receive sizable positive contributions, and therefore is favored by EWPT. Both cases, however, predict $c_R = 0$, so the only way to test this possibility is by effects coming from c_{4t} (four-top physics).

B. One-loop contributions to $Zb\bar{b}$

Although the coupling $Zb\bar{b}$ is not modified at the tree level, it can receive corrections at the one-loop level due to loops of SM particles and custodians that break the custodial and P_{LR} symmetry protecting this coupling. Here we only present the one-loop corrections to $Zb_L\bar{b}_L$ proportional to c_{4q}; they are, as we will see, the only one that can be parametrically larger than the corrections to $\hat{T}$, and then can put, in certain cases, stronger constrains on composite tops.[7] In the limit $M_\rho \gg M_{q^*} \gg m_t$, we find, for both cases of Table I,

$$\delta g_{b_L} = -\delta g_{b_L}^{\rm SM} 3 c_{4q} \xi \left[c_L \xi \left(\frac{4}{\epsilon_t} \log \frac{M_\rho^2}{M_{q^*}^2} + 4 \log \epsilon_t \right) + 2 \log \epsilon_t \right], \tag{46}$$

where

$$\delta g_{b_L}^{\rm SM} = \frac{g}{\cos\theta_W} \frac{m_t^2}{16\pi^2 v^2} \simeq 2 \times 10^{-3}, \tag{47}$$

corresponds to the top one-loop leading contribution to $Zb\bar{b}$ in the SM. Notice that Eq. (46) shows contributions that grow with the custodian mass and are logarithmically sensitive to the heavy resonance mass M_ρ. Therefore, for a composite q_L, where $c_{4q} \sim c_L \sim 1$, these contributions to $Zb\bar{b}$ can be larger than those to $\hat{T}$ for case (a). For example, for $c_{4q} \sim -1/6$, $c_L \sim -0.2$, $\xi \sim 1/4$, and $M_\rho \sim 2.3$ TeV, $M_{q^*} \sim 800$ GeV, the contributions to $\hat{T}$ are below the experimental bound but we find $\delta g_{b_L}/g_{b_L} \sim 0.013$ that is larger than the experimental constraint $-0.002 \lesssim \delta g_{b_L}/g_{b_L} \lesssim 0.006$. These sizable contributions to $Zb\bar{b}$, however, scale with $c_{4q} c_L \propto (y_L/g_\rho)^6$, while those to $\hat{T}$ are proportional to $c_L^2 \propto (y_L/g_\rho)^4$; therefore the contributions to $Zb\bar{b}$ can be parametrically suppressed with respect to those to $\hat{T}$ if y_L is slightly smaller than g_ρ. For a composite t_R, contributions to $Zb\bar{b}$ proportional to the custodian mass or logarithmically sensitive to M_ρ are not present, and therefore Fig. 6 will not suffer large modifications.

For very light custodians, the constraints from $Zb\bar{b}$ can be as important as those from $\hat{T}$ [15,16]. This implies that the allowed low-M_{q^*} regions of Figs. 2 and 6 could be slightly reduced by the $Zb\bar{b}$ constraints. We leave this calculation for a future publication.

V. PHENOMENOLOGICAL IMPLICATIONS AT FUTURE COLLIDERS

In this section we want to study the experimental implications of having one of the top chiralities being a composite state. For this purpose, the effective Lagrangian of Sec. III gives a useful model-independent parametrization of the composite-top new interactions. We

[7] This can be seen by inspection of the one-loop diagrams contributing to $Zb_L\bar{b}_L$ in the effective theory given in Sec. III. Loop diagrams involving c_{4q} and c_L are quadratically divergent.

will not consider physics involving the Higgs that has been already studied in Ref. [5], and we will only concentrate on top physics.

A. Anomalous couplings

The coefficients $c_L^{(1),(3)}$ and c_R give rise to new contributions to the top coupling to the SM gauge bosons. In particular, for the $Zt_L\bar{t}_L$, $Wt_L\bar{b}_L$, and $Zt_R\bar{t}_R$ couplings, we have, respectively,

$$\frac{\delta g_{Zt_Lt_L}}{g_{Zt_Lt_L}} = \frac{(c_L^{(3)} - c_L^{(1)})\xi}{1 - \frac{4}{3}\sin^2\theta_W}, \qquad \frac{\delta g_{Wt_Lb_L}}{g_{Wt_Lb_L}} = c_L^{(3)}\xi, \qquad \frac{\delta g_{Zt_Rt_R}}{g_{Zt_Rt_R}} = \frac{3c_R\xi}{4\sin^2\theta_W}. \tag{48}$$

In the framework considered here we have $c_L^{(3)} \simeq -c_L^{(1)}$ and $c_R \simeq 0$, and therefore only deviations on the t_L couplings can be sizable. To observe these deviations is not going to be easy. At the LHC, top quarks are mostly produced in pairs via the strong gluon fusion process $gg \to t\bar{t}$, decaying to Wb. To measure the Wt_Lb_L coupling, however, a single top must be mostly detected from the process $ub \to dt$. At the LHC this coupling could be measured with a sensitivity around 7% [17], implying that one could see deviations if $c_L\xi \gtrsim 0.07$. For the $Zt\bar{t}$ coupling the situation is more difficult, since it will not be able to be measured at the LHC. The ILC, however, will be the suitable machine to unravel the composite nature of the top. Studies show that the top couplings could be measured with an accuracy as low as 1% [18].

The operators of Sec. III are the dominant ones in a p^2/f^2 expansion. Nevertheless, there are other operators that, although subleading, can have an important impact in future experiments. For a composite t_R one of these subleading operators is

$$\frac{ic_{RR}}{f^2}\frac{y_b}{y_t}H^\dagger D_\mu \tilde{H}\bar{b}_R\gamma^\mu t_R, \tag{49}$$

where, due to the presence of the b_R, the coefficient of the operator is suppressed by the Yukawa coupling of the bottom $y_b/y_t \simeq 0.02$. The coupling c_{RR} is constrained by $b \to s\gamma$ to be $c_{RR}\xi \lesssim 0.2$ [19]. At the LHC this coupling will be able to be tested in top decays. Reference [20] gives a precision $-3.2 \lesssim c_{RR}\xi \lesssim 6.8$ for an integrated luminosity of $L = 10\ \text{fb}^{-1}$.

Another subleading operator is

$$\frac{c_M y_t}{16\pi^2 f^2}\bar{q}_L W^{\mu\nu}\tilde{H}\sigma^{\mu\nu}t_R, \tag{50}$$

where $W^{\mu\nu}$ is the field strength of the SM W boson. Reference [20] gives a precision for this coupling at the LHC of order $-3.6 \lesssim c_M\xi \lesssim 3.6$ for $L = 10\ \text{fb}^{-1}$. Similar coupling for the gluon could be measured at the LHC with an accuracy of $c_M\xi \simeq 0.4$ for $L = 100\ \text{fb}^{-1}$ [17].

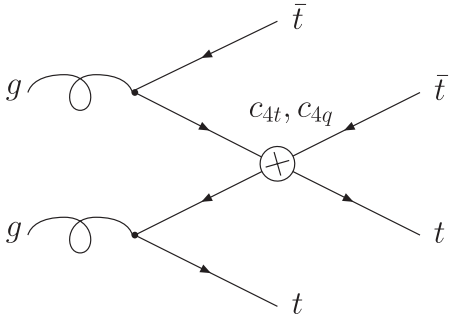

FIG. 7. Contribution of the four-top interaction to the process $pp \to t\bar{t}t\bar{t}$.

B. Four-top interactions and $pp \to t\bar{t}t\bar{t}(b\bar{b})$

The most genuine effect of a composite top comes from the four-top interaction of Eqs. (11) and (15). For a composite t_R the operator $\mathcal{O}_{4t} = (\bar{t}_R\gamma^\mu t_R)(\bar{t}_R\gamma_\mu t_R)$ induces a top-scattering amplitude that grows with the energy

$$|\mathcal{A}(t_R\bar{t}_R \to t_R\bar{t}_R)|^2 = 64\frac{c_{4t}^2}{f^4}(u - 2m_t^2)^2. \tag{51}$$

Similar expression holds for a composite t_L, induced in this case by the operator $\mathcal{O}_{4q} = (\bar{q}_L\gamma^\mu q_L)(\bar{q}_L\gamma_\mu q_L)$. The growth with the energy of the four-top interaction will lead at the LHC to an enhancement of the cross section for $pp \to t\bar{t}t\bar{t}$ as shown in Fig. 7. We have calculated the total cross section for the process $pp \to t\bar{t}t\bar{t}$ using the MadGraph/MadEvent generator [21]. For the computation we have used the CTEQ6M parton distribution functions and $Q = 1$ TeV as a reference value of the QCD renormalization and factorization scales. The result as a function of c_{4t} is shown in Fig. 8 for $f = 500$ GeV. When the operator $\mathcal{O}_{4t}$ is generated by a heavy color resonance, Eq. (17), the total cross section for $pp \to t\bar{t}t\bar{t}$ is smaller than the SM one. Nevertheless, this cross section can be substantially larger for larger values of c_{4t}. Similar results have been presented previously in Ref. [22].

Because of Eq. (51), we expect the $t\bar{t}$ pair coming from the four-top interaction to have a larger transverse mo-

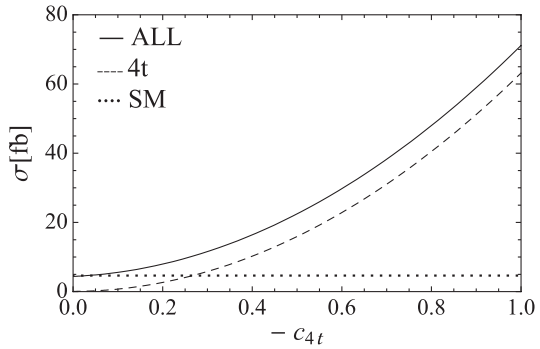

FIG. 8. Cross section for $pp \to t\bar{t}t\bar{t}$ as a function of c_{4t} arising from the operator $\mathcal{O}_{4t}$ (4t), SM diagrams (SM) and both (ALL).

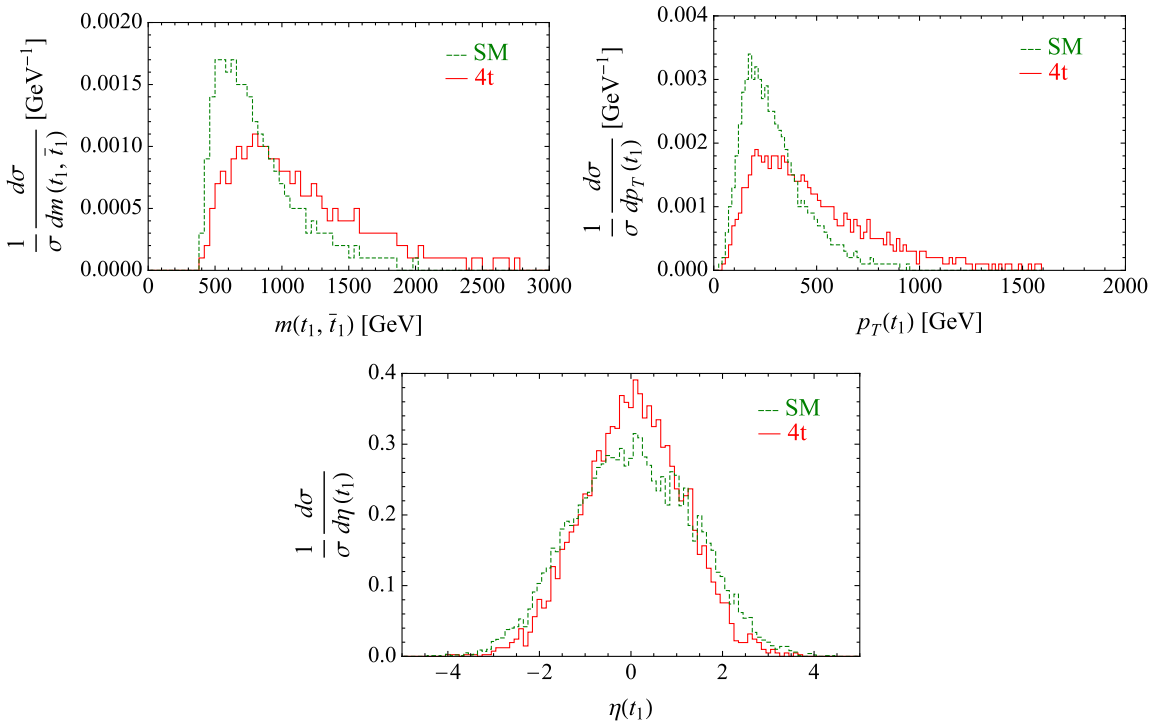

FIG. 9 (color online). Normalized differential cross section for $pp \to t\bar{t}t\bar{t}$ arising from the operator $\mathcal{O}_{4t}$ and the SM plotted versus the invariant mass of the scattered top pair $m(t_1, \bar{t}_1)$, the transverse momentum $p_T(t_1)$, and the pseudorapidity $\eta(t_1)$.

menta than those coming from gluons. Hence, by taking $p_T(t_1) > p_T(t_2)$ (and the same for the antitops), we can identify the top t_1 as the scattered top and the top t_2 as the spectator top. We also expect the $t_1\bar{t}_1$ pair to have large invariant mass m and to be produced at large angles and then to have a small pseudorapidity η. These observables can be useful to discriminate the four-top signal versus backgrounds.

In Fig. 9 we plot the four-top normalized differential cross section arising from the four-top contact interaction, and compare this with that of the SM. We show the normalized differential cross section versus the invariant mass of the scattered top pair $m(t_1, \bar{t}_1)$, the transverse momentum of t_1, $p_T(t_1)$, and its pseudorapidity $\eta(t_1)$; being normalized distributions, they do not depend on c_{4t} or f. As expected, the normalized differential cross sections due to the new four-top contact interaction are larger for large $m(t_1, \bar{t}_1)$, $p_T(t_1)$ or small $\eta(t_1)$ than those of the SM. In Table II we give the values of the cross section for the four-top production for different cuts in the top-pair invariant mass, transverse momenta, or pseudorapidities. We have taken $c_{4t} = -1/6$ and $f = 500$ GeV, corresponding to the values of the composite Higgs model, Eqs. (4) and (17), respectively. For the different cuts we give the value of the significance taken as $\mathcal{S} = \frac{\sigma_{\rm ALL} - \sigma_{\rm SM}}{\sqrt{\sigma_{\rm SM}}} \times \sqrt{L}$, where L is the integrated luminosity that we take to be $L = 100$ fb^{-1}. We see that the cuts do not substantially increase the significance. Nevertheless, these cuts can be useful in order to eliminate reducible backgrounds, since the detection of the four tops will crucially depend on how well one will be able to reconstruct them at LHC. Since the scattered tops are very energetic, their decay products will be highly collimated, making conventional reconstruction algorithms difficult to apply. In Ref. [22] an analysis at the particle level of the process $pp \to t\bar{t}t\bar{t}$ has been made, adopting the simple signature of at least two like-sign

TABLE II. Cross section for $pp \to t\bar{t}t\bar{t}$ arising from $\mathcal{O}_{4t}$ with $c_{4t} = -1/6$ and $f = 500$ GeV ($4t$), SM diagrams (SM) and both (ALL) for different cuts. The corresponding significance $\mathcal{S}$ is also given.

	Cuts	σ_{4t} [fb]	$\sigma_{\rm SM}$ [fb]	$\sigma_{\rm ALL}$ [fb]	$\mathcal{S}$
(a)	no cuts	1.8	4.6	7.0	11
(b)	$m(t_1, \bar{t}_1) > 650$ GeV	1.5	2.8	4.5	10
(c)	$p_T(t_1), p_T(\bar{t}_1) > 200$ GeV, $p_T(t_2), p_T(\bar{t}_2) > 30$ GeV	1.3	2.2	3.5	8.7
(d)	$\lvert\eta\rvert(t_1), \lvert\eta\rvert(\bar{t}_1) < 2$, $\lvert\eta\rvert(t_2), \lvert\eta\rvert(\bar{t}_2) < 4$	1.5	3.5	5.4	10
(e)	(b) + (c) + (d)	1.1	1.7	2.8	8.4

TABLE III. Cross section for $pp \to t\bar{t}b\bar{b}$ arising from $\mathcal{O}_{4q}$ with $c_{4q} = -1/6$ and $f = 500$ GeV ($4q$), SM diagrams (SM) and both (ALL) for different cuts. The corresponding significance $\mathcal{S}$ is also given.

	Cuts	σ_{4q} [fb]	$\sigma_{\rm SM}$ [fb]	$\sigma_{\rm ALL}$ [fb]	$\mathcal{S}$
(a)	$p_T(b)$, $p_T(\bar{b}) > 150$ GeV + $\Delta R(b, \bar{b}) > 1$	5.6	16	23	18
(b)	(a) + $m(t, \bar{t}) > 600$ GeV	3.9	6.0	11	19
(c)	(a) + $m(b, \bar{b}) > 600$ GeV	3.9	4.4	9.1	23
(d)	(a) + $p_T(t)$, $p_T(\bar{t}) > 300$ GeV	1.3	1.2	2.6	13

leptons $l^{\pm}l'^{\pm}$ plus at least two hard jets. They get significances $\sim$5 for a value of $c_{4t} \sim 1/6$ and $f \sim 300$–450 GeV. A more extended analysis at the detector level will be needed to study the feasibility of detecting this process.

In the case of a composite q_L, the operator $\mathcal{O}_{4q}$ also induces an amplitude for the process $b\bar{b} \to t\bar{t}$ that grows with the energy

$$|\mathcal{A}(b_L\bar{b}_L \to t_L\bar{t}_L)|^2 = 4\frac{c_{4q}^2}{f^4}(u - m_t^2 - m_b^2)^2. \quad (52)$$

At the LHC this will give an enhancement of the cross section of $pp \to t\bar{t}b\bar{b}$ similar to Fig. 7 but with b either as the spectator or the scattered quarks. To calculate with the MadGraph/MadEvent generator the total cross section for $pp \to t\bar{t}b\bar{b}$ we will demand a large p_T for the bottom quarks and a large separation angle between them, in order to avoid large logarithmic corrections due to collinear $b\bar{b}$ coming from the gluon [23].[8] In Table III we give the cross section for $pp \to t\bar{t}b\bar{b}$ for $p_T(b)$, $p_T(\bar{b}) > 150$ GeV and $\Delta R(b, \bar{b}) = \sqrt{(\eta_b - \eta_{\bar{b}})^2 + (\phi_b - \phi_{\bar{b}})^2} > 1$ where ϕ_i is the azimuthal angle (we take the renormalization scale $Q = 0.5$ TeV, $c_{4q} = -1/6$, and $f = 500$ GeV). To show the dependence of the $t\bar{t}b\bar{b}$ production cross section versus the invariant mass, transverse momentum, and pseudorapidity of the bottom and top, we plot in Fig. 10 the normalized differential cross sections for $pp \to t\bar{t}b\bar{b}$ induced by the four-fermion interaction, and compare them with the SM ones. The variation of the cross section and the significance of the signal for several cuts is given in Table III.

The determination of the top-quark polarization gives a complementary way to probe the properties of the top interactions and to discriminate between either right-handed or left-handed top compositeness. At the LHC, the top quarks are dominantly produced unpolarized by QCD interactions. In the presence of the operators $\mathcal{O}_{4t,4q}$, however, the $t\bar{t}t\bar{t}$ production yields an excess of either right- or left-handed scattered tops that can be visible by measuring the top polarization.

The polarization of the top quarks can be analyzed from the angular distribution of their decay products. In the decay channel $t \to W^+b \to l^+\nu b$, $q\bar{q}'b$, the angular distribution of the "spin analyzers" $X = l^+$, ν, q, $\bar{q}'$, W^+, b is given by

$$\frac{1}{\Gamma}\frac{d\Gamma}{d\cos\theta_X} = \frac{1}{2}(1 + \alpha_X \cos\theta_X), \quad (53)$$

with θ_X being the angle between the direction of X (in the top rest frame) and the direction of the top polarization. The constants $\alpha_X \in [-1, 1]$, take in the SM the approximate values $\alpha_{l^+} = \alpha_{\bar{d}} = 1$, $\alpha_\nu = \alpha_u = -0.32$, $\alpha_{W^+} = -\alpha_b = 0.41$ [24]. From Eq. (53) we can obtain the top production differential cross section

$$\frac{1}{\sigma}\frac{d\sigma}{d\cos\theta_X} = F_R + F_L = \frac{A}{2}(1 + \alpha_X \cos\theta_X) + \frac{1 - A}{2}(1 - \alpha_X \cos\theta_X), \quad (54)$$

where F_R and F_L are, respectively, the angular distributions for right- and left-handed quarks and A corresponds to the fraction of right-handed quarks produced (therefore $A \in [0, 1]$). In the SM we expect $A \sim 1/2$. In Fig. 11 we show the normalized differential cross section for four-top production at the LHC as a function of $\cos\theta_X$ where $X = l^+$ is the lepton coming from the top with the highest p_T. We show this for tops arising either from $\mathcal{O}_{4t}$ ($4t$) or $\mathcal{O}_{4q}$ ($4q$), and compare with the SM case. By fitting Fig. 11 with the distribution Eq. (54) we find $A \simeq 0.5$ for the SM, while $A \simeq 0.8$ and 0.2, respectively, for the $4t$ and $4q$ case. From Eq. (54) one can calculate forward-backward asymmetries in the lepton channel similar to those of Ref. [25] that can be useful to disentangle the helicity of the top if an excess in the four-top production is found at the LHC.

VI. CONCLUSIONS

In models in which EWSB is triggered by a new strong sector or a warped extra dimension, the SM fermions can get their masses by mixing with composite states (or operators) of the new sector. In this framework it is natural to consider due to the heaviness of the top that one of its chiralities, q_L or t_R, is mostly composite.

[8] Alternatively, we could sum up these large logarithmic terms by introducing the b quark parton distribution functions and calculating the process $pp \to t\bar{t}$. Nevertheless, the huge SM contribution to top-pair production would in this case swamp the effect of a composite top coming from Eq. (52). We thank Tim Tait for pointing out these problems to us.

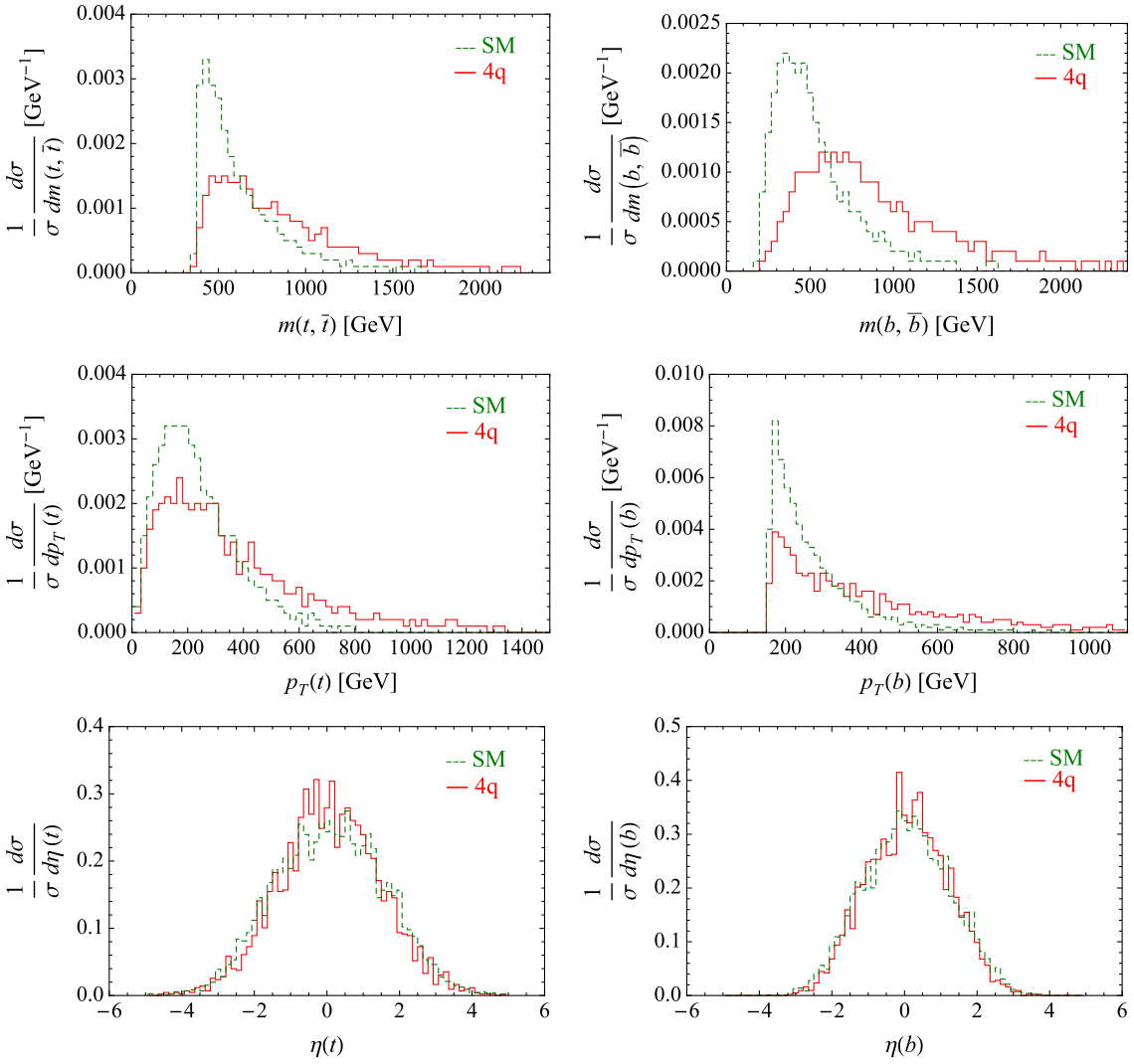

FIG. 10 (color online). Normalized differential cross section for $pp \to t\bar{t}b\bar{b}$ [with cuts $p_T(b)$, $p_T(\bar{b}) > 150$ GeV and $\Delta R(b,\bar{b}) > 1$] induced by the operator $\mathcal{O}_{4q}$ versus the invariant mass, the transverse momentum, and the pseudorapidity of the tops or bottoms. We compare them with those of the SM.

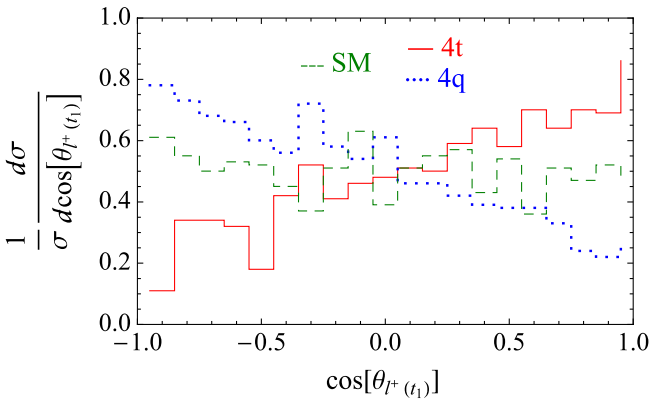

FIG. 11 (color online). Normalized differential cross section for $pp \to t\bar{t}t\bar{t}$ versus $\cos\theta_X$ where X is the lepton coming from the decay of the scattered top.

In this article we have seen that present experimental bounds do not rule out this possibility. The custodial symmetry of the BSM sector plays an important role guaranteeing that the T parameter and $Zb\bar{b}$ do not get corrections at tree level for the cases (a) and (b) of Table I. We have calculated the one-loop effects to the T parameter and showed, for a composite q_L, that while in case (b) the bounds from $\hat{T}$ are very restrictive (Fig. 4), for case (a), the presence of the custodial partners of the top, the custodians, avoids large one-loop contributions to $\hat{T}$ (Fig. 2). For a composite t_R the bounds from $\hat{T}$ are very weak; case (a) does not generate contributions to $\hat{T}$, while for case (b) one finds wide allowed regions (Fig. 6). Our one-loop calculation shows that moderate and positive contributions to $\hat{T}$ are more probable in regions in which the coefficients of the higher-dimensional operators c_i are negative. These regions, although absent in minimal holo-

graphic models [15], can be present in more generic scenarios. These positive contributions to $\hat{T}$ are needed in this class of models in order to accommodate a generic positive contribution to the S parameter.

At future accelerators, we have seen that top compositeness can be tested by looking for deviations on the $Zt\bar{t}$ and $Wt\bar{b}$ coupling. Only the second one, however, can be measured with certain accuracy at the LHC. The ILC would clearly be an excellent machine to probe the properties of the top and determine its degree of compositeness. A second important effect of top compositeness is the presence of four-top contact terms that enhances the cross section for $pp \to t\bar{t}t\bar{t}$ at high energies. We have calculated the cross section of this process at the LHC for the case of a composite t_R, and showed several observables that can allow us to discriminate from the SM prediction. It is however unclear, due to the smallness of the cross section, whether the four-top production can be seen at the LHC. Clearly, a more detailed analysis is needed to assure the feasibility of this process. Similar analysis has been discussed for the process $pp \to t\bar{t}b\bar{b}$ for the case of a composite q_L.

We finalize saying that the composite nature of the top could also be seen indirectly by detecting the custodians. Studies in this direction have been recently carried out in Ref. [26].

ACKNOWLEDGMENTS

This work was partly supported by the FEDER Research Project No. FPA2005-02211 and DURSI Research Project No. SGR2005-00916. The work of J. S. was also supported by the Spanish MEC FPU Grant No. AP2006-03102.

[1] S. Weinberg, Phys. Rev. D **13**, 974 (1976); **19**, 1277 (1979); L. Susskind, Phys. Rev. D **20**, 2619 (1979).
[2] D. B. Kaplan and H. Georgi, Phys. Lett. **136B**, 183 (1984); **136B**, 187 (1984); M. J. Dugan, H. Georgi, and D. B. Kaplan, Nucl. Phys. **B254**, 299 (1985).
[3] C. Csaki, C. Grojean, L. Pilo, and J. Terning, Phys. Rev. Lett. **92**, 101802 (2004); Y. Nomura, J. High Energy Phys. 11 (2003) 050; R. Barbieri, A. Pomarol, and R. Rattazzi, Phys. Lett. B **591**, 141 (2004).
[4] K. Agashe, R. Contino, and A. Pomarol, Nucl. Phys. **B719**, 165 (2005).
[5] G. F. Giudice, C. Grojean, A. Pomarol, and R. Rattazzi, J. High Energy Phys. 06 (2007) 045.
[6] M. E. Peskin and T. Takeuchi, Phys. Rev. D **46**, 381 (1992).
[7] K. Agashe, R. Contino, L. Da Rold, and A. Pomarol, Phys. Lett. B **641**, 62 (2006).
[8] R. Contino, T. Kramer, M. Son, and R. Sundrum, J. High Energy Phys. 05 (2007) 074.
[9] D. B. Kaplan, Nucl. Phys. **B365**, 259 (1991).
[10] R. Contino, L. Da Rold, and A. Pomarol, Phys. Rev. D **75**, 055014 (2007).
[11] R. S. Chivukula, S. B. Selipsky, and E. H. Simmons, Phys. Rev. Lett. **69**, 575 (1992).
[12] R. Barbieri, A. Pomarol, R. Rattazzi, and A. Strumia, Nucl. Phys. **B703**, 127 (2004).
[13] A. G. Cohen, H. Georgi, and B. Grinstein, Nucl. Phys. **B232**, 61 (1984).
[14] D. C. Kennedy, Phys. Lett. B **268**, 86 (1991).
[15] M. S. Carena, E. Ponton, J. Santiago, and C. E. M. Wagner, Phys. Rev. D **76**, 035006 (2007).
[16] R. Barbieri, B. Bellazzini, V. S. Rychkov, and A. Varagnolo, Phys. Rev. D **76**, 115008 (2007); P. Lodone, arXiv:0806.1472.
[17] G. Weiglein *et al.* (LHC/LC Study Group), Phys. Rep. **426**, 47 (2006).
[18] J. A. Aguilar-Saavedra *et al.* (ECFA/DESY LC Physics Working Group), arXiv:hep-ph/0106315.
[19] F. Larios, M. A. Perez, and C. P. Yuan, Phys. Lett. B **457**, 334 (1999).
[20] J. A. Aguilar-Saavedra, J. Carvalho, N. Castro, F. Veloso, and A. Onofre, Eur. Phys. J. C **50**, 519 (2007); **53**, 689 (2008).
[21] F. Maltoni and T. Stelzer, J. High Energy Phys. 02 (2003) 027; J. Alwall *et al.*, J. High Energy Phys. 09 (2007) 028.
[22] B. Lillie, J. Shu, and T. M. P. Tait, J. High Energy Phys. 04 (2008) 087.
[23] W. Bernreuther, J. Phys. G **35**, 083001 (2008).
[24] F. Hubaut, E. Monnier, P. Pralavorio, K. Smolek, and V. Simak, Eur. Phys. J. C **44S2**, 13 (2005).
[25] K. Agashe, A. Belyaev, T. Krupovnickas, G. Perez, and J. Virzi, Phys. Rev. D **77**, 015003 (2008).
[26] R. Contino and G. Servant, J. High Energy Phys. 06 (2008) 026.